

Characterization of Fe-ACF/TiO₂ composite and photocatalytic activity for MB Solution under visible light

Kan Zhang, Ze-Da Meng and Won-Chun Oh*

*Department of Advanced Materials & Science Engineering, Hanseo University,
Chungnam 356-706, Korea*

(Received June 2, 2009; Accepted April 21, 2010)

Fe-ACF/TiO₂ 복합체의 특성화와 가시광선조건에서 MB 용액의 광촉매활성

장 간 · 맹척달 · 오원춘*

한서대학교, 신소재공학과
(2009. 6. 2. 접수, 2010. 4. 21. 승인)

Abstract: In present study, a conventional sol-gel method was used to prepare Fe-ACF/TiO₂ composites, a kind of composite photocatalysts, whose capability was evaluated by degrading methylene blue (MB) solution. The particle size, surface structure, crystal phase and elemental identification of the composites prepared were characterized by BET, SEM, XRD and EDX, respectively. The spectra of MB concentration degraded under visible light were obtained by UV/Vis spectrophotometer. These obtained spectra demonstrated the photocatalytic activity from removal concentrations of MB. It was considered that these photonic activities are induced by a strong synergetic reaction among ACF, TiO₂ and Fe in the composite photocatalysts under visible light.

요약: 본 연구에서 종래의 졸-겔법을 사용하여 Fe-ACF/TiO₂ 광촉매 복합체를 제조하였고, 이들 광촉매의 분해능은 메틸렌블루 (MB) 용액의 분해에 의하여 나타내었다. 제조된 이들 복합체에 대한 입자크기, 표면구조, 결정상 및 원소분석을 BET, SEM, XRD 및 EDX에 의하여 각각 특성화 하였다. 가시광선 조건에서 분해된 MB 농도에 대한 스펙트라는 UV/Vis 분광기에 의하여 얻어 졌다. 이와 같이 얻어진 스펙트라는 MB의 제거된 농도로부터 광촉매 활성을 입증하였다. 이들 광촉매 활성은 가시광선 조건에서 복합체 광촉매 내에 존재하는 ACF, TiO₂ 및 Fe 사이에 강력한 시너지 반응에 의해 유도된 것으로 여겨진다.

Key words: Fe-ACF/TiO₂ composite, methylene blue, photo-Fenton, XRD

★ Corresponding author

Phone : +82-(0)41-660-1337 Fax : +82-(0)41-688-3352

E-mail : wc_oh@hanseo.ac.kr

1. Introduction

Due to its low cost, chemical stability, non-toxicity and complete mineralization,¹⁻⁵ titania has been extensively employed as heterogeneous photocatalytic material for solving environmental problems,⁶⁻⁹ especially for eliminating organic dyes in wastewater. These organic dyes can be degraded easily because TiO₂ is subjected to photocatalytic oxygenation owing to the resulted photonic activity. When some electrons may jump from the valence band to the conduction band, some photoholes will be generated as well as electrons. The hole and electron are powerful oxidizing and reducing agents respectively. The photochemical phenomena can be widely occurred on the surface of TiO₂ under ultraviolet (UV) irradiation, which was attributed that surface TiO₂ can be excited with light illumination of suitable wavelength ($\lambda < 390$ nm or $E_{bg} = 3.2$ eV).¹⁰⁻¹⁴ However, UV light seemed to be a difficult condition in degradation of mass wastewater. Therefore, effective utilization of visible light to degrade the dye pollutants from the viewpoint of using the solar energy is an attractive attempt,¹⁵ the major drawback in the practical application under irradiation of natural solar light is lower energy (3.2 eV) for TiO₂ particles due to use of only approximately 4% of the solar radiation.¹⁶ It implied that electron energy is low under visible light. Then, multifarious efforts have been made to extend the light absorption of the photocatalysts to the visible region.¹⁷⁻¹⁹ For example, TiO₂ treated with different transition metals such as Ce²⁰ and Nd²¹ can effectively improve above defects. The fact was considered that the transition metal ions modified TiO₂ particles can narrow the band gap or introduce intra-band gap energy states, hereby increasing the photonic activity.²² Transition metal as iron in the TiO₂ lattices can carry photogenerated electrons and fabricate photo-fenton reaction. Photonic activity may be enhanced due to iron assistance in TiO₂ under the visible light. Nevertheless, iron ions often behave as recombination centers for the photogenerated charged carriers. The defect has been widely reported in the previous work.^{23,24}

In this paper, Fe and TiO₂ were immobilized on modified ACF surface by a sol-gel method due to the higher surface area of ACF.^{25,26} The Fe-ACF/TiO₂ composites were characterized by BET, SEM, XRD and EDX. The successful product was named Fe-ACF/TiO₂ composite photocatalyst. The photonic activity of the Fe-ACF/TiO₂ is evaluated by the photodegradation efficiency of MB under visible light.

2. Experimental Procedure

2.1. Materials

Activated Carbon Fiber (ACF) was purchased from EAST ASIS Carbon Fibers Co., Ltd, Anshan, China. Titanium (IV) oxysulfate hydrate (TiOSO₄·xH₂O (TOS), Sigma-Aldrich, Germany) was selected as a titanium source for the preparation of ACF/TiO₂ composites, and Fe(NO₃)₃·9H₂O as the ferric source was purchased from Duksan Pure Chemical Co. (99+%, ACS reagent, Korea). The MB was used as analytical grade which was purchased from Duksan Pure Chemical Co., Ltd, Korea.

2.2. Preparation of samples

In this experimental process, first, 10 g ACF powder was added into to 50 mL 0.1, 0.25 and 0.5 M Fe(NO₃)₃·9H₂O solution and the mixtures were stirred 24 h using a non-magnetic stirrer at room temperature. After heat treatment at 773 K, we obtained the Fe-ACF. The Fe-ACF was put into the mixture of TOS and ethanol. Then the mixed solution was stirred for 5 h in an air atmosphere. After stirring solution was transformed to gel state, and these gels were heat treated at 923 K for 1h. And then the Fe-treated ACF/TiO₂ composites were obtained. The nomenclatures of prepared samples are listed in *Table 1*. At

Table 1. Nomenclatures of non-treated ACF/TiO₂ and Fe-treated ACF/TiO₂ composites

Samples	Nomenclatures
ACF+ Titanium iso propoxide	FT0
ACF+ 0.1M Fe(NO ₃) ₃ + 1M TOS/alcohol	FT1
ACF+ 0.25M Fe(NO ₃) ₃ + 1M TOS/alcohol	FT2
ACF+ 0.5M Fe(NO ₃) ₃ + 1M TOS/alcohol	FT3

the same time, an original data of ACF/TiO₂ was quoted from former experiment²⁷ and compared with that of Fe-ACF/TiO₂ composites obtained in present study.

2.3. Characteristics and investigations of the samples

The BET surface area by N₂ adsorption method was measured at 77 K using a BET analyzer (MONOSORB, USA). XRD (Shimadzu XD-D1, Japan), the result was used to identify the crystallinity by Cu K α radiation. SEM was used to observe the surface state and structure of Fe-ACF/TiO₂ composites using a JSM-5200 JOEL electron microscope (Japan). EDX spectra were also obtained for determining the elemental information of Fe-ACF/TiO₂ composites. UV-vis spectra for degrading MB solution by Fe-ACF/TiO₂ composites under visible lamp irradiation were recorded using a Genspec III (Hitachi, Japan) spectrometer. Used an 8W LED lamp ($\lambda > 420$ nm, Fawoo Technology, Korea) as visible light source was adopted to irradiate the MB solutions.

2.4. Photocatalytic activity of Fe-ACF/TiO₂

The photochemical behavior was recorded using preparation of Fe-ACF/TiO₂ composites in a 100 mL glass container and respectively irradiating the system with the Solar Simulator (visible light 8W). The initial concentration of MB was chosen 1.0×10^{-5} mol/L. The amount of suspended composites was kept at 0.6 g/L in 50 mL MB solution. Then, the solution mixed with composites was emplaced in the dark for at least 2 h in order to establish an adsorption-desorption equilibrium, which was hereafter considered as the initial concentration (c_0) after dark adsorption. Then, the reactor was placed under visible light. Solution was then withdrawn regularly from the reactor by an order of 0 min, 30 min, 60 min, 90 min, and 120 min, afterwards, 10 mL of solution was taken out and immediately centrifuged to separate any suspended solid. The clean transparent solution was analyzed by using a UV-vis spectrophotometer. The full spectrum (200-800 nm) for each sample was recorded.

3. Results and Discussion

3.1. Structure and morphology of Fe-treated ACF/TiO₂

The Fe-treated ACF/TiO₂ composite photocatalysts prepared with different concentration of Fe component were denoted as FT1, FT2 and FT3. The BET surface area of the as-received ACF was 1842 m²/g, it can be evidently seen that there was large change of the micropore size for Fe-ACF/TiO₂ composites compared with that of corresponding ACF.

The data of these surface areas are summarized in Table 2. This result indicated that the total surface area decreased after formation of TiO₂ particles on the ACF surface. It was considered that the invaded Ti particles can be blocked to pore in ACF. It also noteworthy decreases of surface area as another means of improving photocatalytic activity. Otherwise, the BET surface area was continuously decreased from FT1 to FT3. The variation of surface parameters was probably caused by the Fe compounds.

Fig. 1 shows the SEM surface morphology of Fe-treated ACF/TiO₂ composites. It showed that the uniform particles indicated in images that were coherent together, and which was beneficial for the photocatalytic reaction. It was considered that the photocatalytic reaction is carried out on the external surfaces of the ACF/TiO₂ composites catalysts. The existed reactants using the nano-size structured catalyst could provide a more effective surface for MB adsorption and light absorption.²⁶ The titanium complex particles more regularly distributed on and around the ACF surfaces with the increase of Fe (NO₃)₃ concentrations. It was considered that a good dispersion of small particles could provide more reactive sites for the reactants. Accordingly, a

Table 2. Specific BET surface areas of pristine material and Fe-treated ACF/TiO₂ composite samples

Sample	S _{BET} (m ² /g)
Pristine ACF	1842
FT1	682
FT2	660
FT3	509

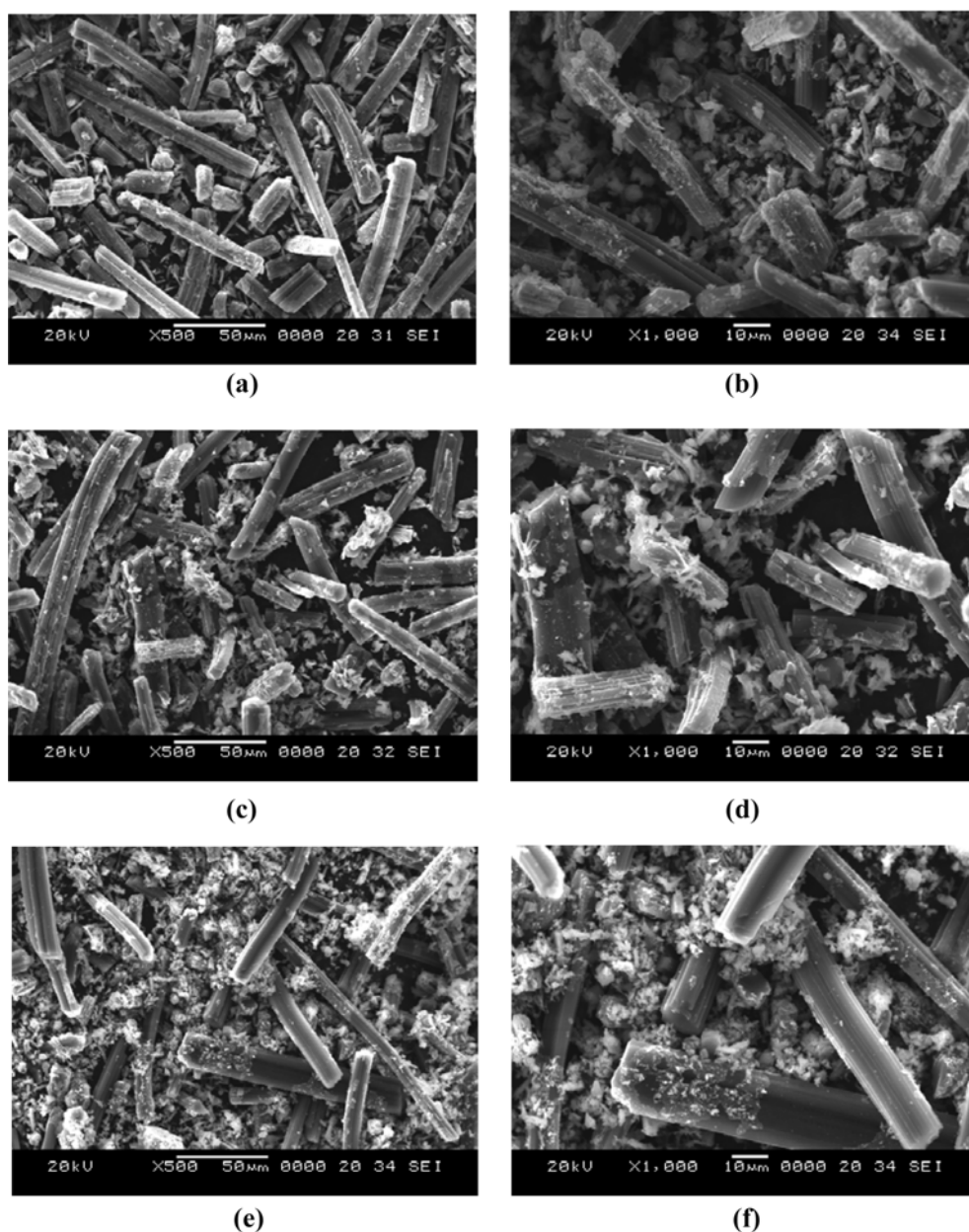


Fig. 1. SEM images of Fe-ACF/TiO₂ composites: FT1: (a) $\times 500$, (b) $\times 1000$; FT2, (c) $\times 500$, (d) $\times 1000$ and FT3 (e) $\times 500$, (f) $\times 1000$.

distribution of TiO₂ particle was expected for a high photocatalytic yield.²⁸ But the particles were partially agglomerated on ACF surface from Fig. 1 images observation, we can see that the surface of Fe-ACF/TiO₂ composites contained defects, which caused by introduction of Fe particles during modification,

which situation might conceal some production of photonic in degradation of MB solution.

The titanium phases in the photocatalysts were identified by X-ray diffraction. The XRD patterns for the Fe-treated ACF/TiO₂ photocatalysts prepared are shown in Fig. 2. The figure showed that distinct

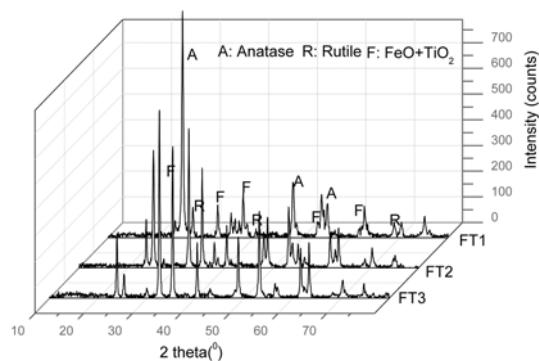
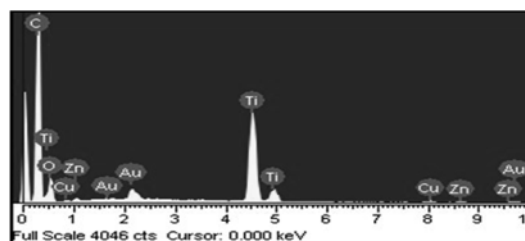


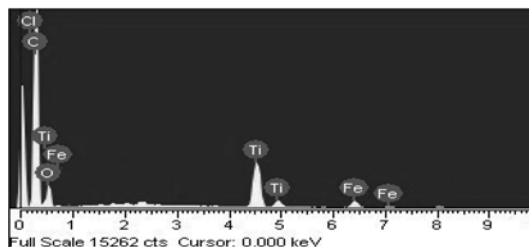
Fig. 2. XRD patterns of powdered Fe-ACF/TiO₂ composites.

anatase and weak rutile phase of TiO₂ were observed in all samples. According to the former study,²⁹ the anatase phase formed below 773 K begin to transform to rutile-type structure above 873 K and changed into single phase of rutile at 973~1173 K. It was well known that the crystal structure of the titanium dioxide is mainly determined by the heat treatment temperature. The peaks at 25.3, 37.8, 48.0, 53.8, 54.9 and 62.5 are the diffractions of (101), (004), (200), (105), (211) and (204) planes of anatase, indicating the developed composites existed in anatase state. There are some peaks also found at 27.4, 36.1, 41.2 and 54.3 that belong to the diffraction peaks of (110), (101), (111) and (211) of rutile. Therefore, it can be concluded that the developed Fe-ACF/TiO₂ composites had a mixture crystal structure, just is anatase and rutile structures. It is agreed with the previous works^{30,31} which prepared C/TiO₂ composites had a mixture structure of anatase and rutile crystals by crystallization when the temperature reached 973 K. However, The TiO₂ crystalline phases were considerably decreased when the amount of Fe was increased. The decrease can be explained an increase of Fe and a decrease of the TiO₂ lattice distance.

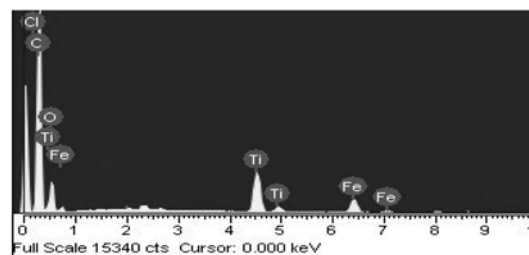
The EDX data of Fe-treated ACF/TiO₂ are shown in Fig. 3. These spectra showed the presence of peaks from the C, O and Ti elements. TiO₂ particles showed a peak around 0.2 keV and another intense peak appears at 4.5 keV. The intense peak is assigned to TiO₂ in the bulk form and the less intense peak is assigned to TiO₂ surface.³² The peaks due to iron were clearly distinct in Fe-ACF/TiO₂ at 7.1 and 6.4



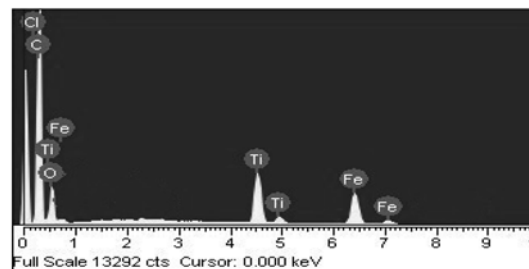
(a)



(b)



(c)



(d)

Fig. 3. EDX elemental microanalysis of non-treated ACF/TiO₂ and Fe-treated ACF/TiO₂ composites: (a) FT0, (b) FT1, (c) FT2 and (d) FT3.

keV. Because of coating by Au for preparation of EDX images, some peaks appear around 9.6 keV were omitted. Elemental composition analyses of the composite series are listed in Table 3. From the Table 3, it was shown that carbon and Ti are present as major elements in the composite series. As expected, it was observed that the Fe contents of Fe-treated

Table 3. EDX elemental microanalysis (wt.%) of non-treated ACF/TiO₂ and Fe-treated ACF/TiO₂ composites

Samples	Elements			
	C	O	Ti	Fe
FT0	53.84	21.79	23.90	0
FT1	67.45	19.08	9.16	2.04
FT2	63.16	22.23	7.59	4.72
FT3	59.78	19.37	8.16	9.57

ACF/TiO₂ composites show an increase with the increase of Fe (NO₃)₃ concentration.

3.2. Photonic activity

The absorbance spectra of MB concentration at 1.0×10^{-5} mol/L against the non-treated ACF/TiO₂ and Fe-treated ACF/TiO₂ composite series are shown in Fig. 4. According to the Fig. 4, the absorbance values decreased with an increase of

irradiation time. From the curves of MB degradation, we can see that a uniform and sharp band of absorption peaks were found at around 660 nm. It implied that analogical reactions were occurred for degrading MB molecule under UV and visible light. Photonic activity can be also produced under visible light. And detailed mechanism of dye degradation under visible light irradiation is described by Eqs. ((1)-(6))

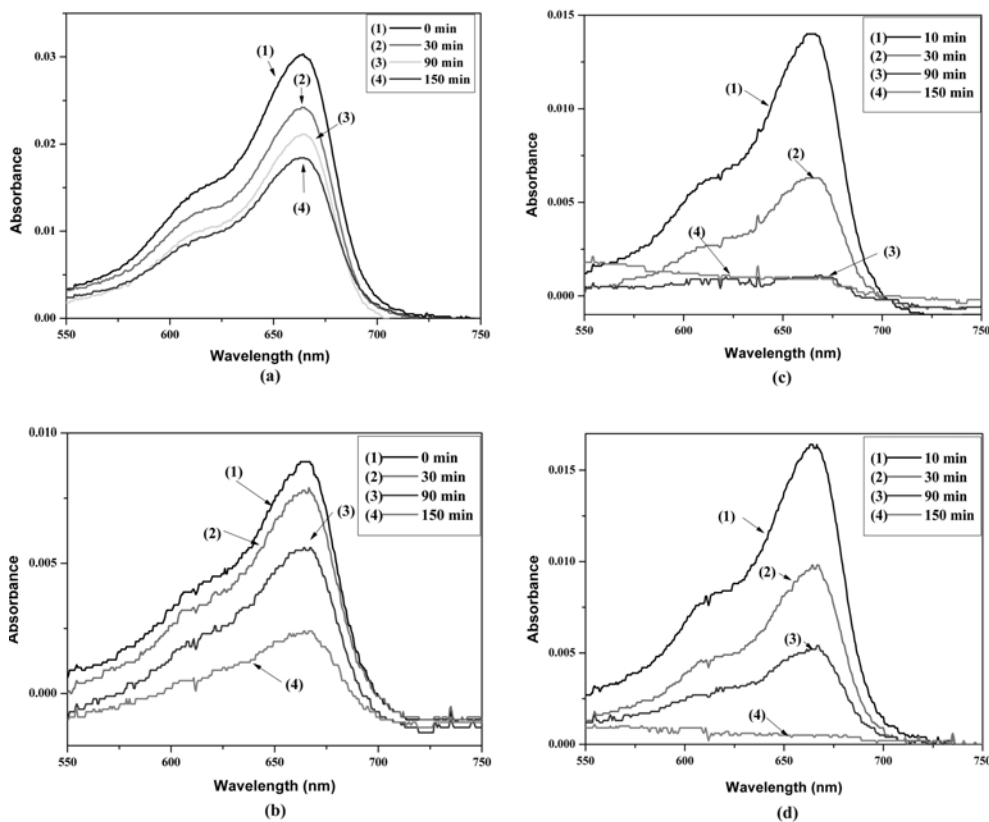
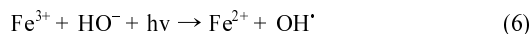
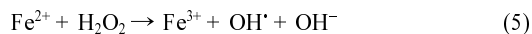
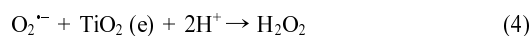
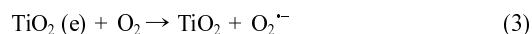
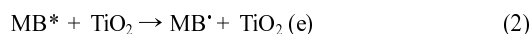


Fig. 4. UV/Vis spectra of MB concentration against the Fe-ACF/TiO₂ composite under various time conditions: (a) FT0, (b) FT1, (c) FT2 and (d) FT3.

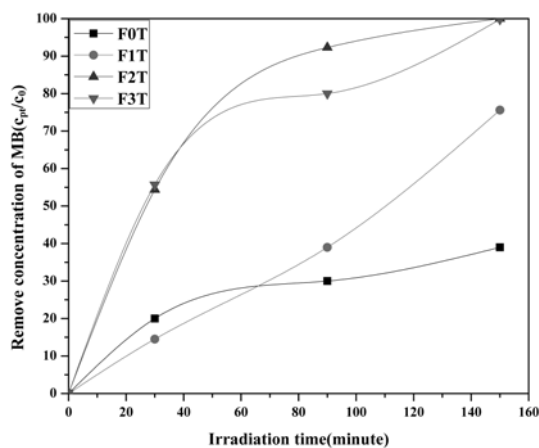
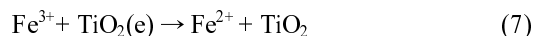


Fig. 5. Dependence of removal concentration of MB in the aqueous solution c_p/c_0 on irradiation time for the ACF/TiO₂ under UV and Fe-ACF/TiO₂ composites under visible light.

Fig. 5 shows a comparison of photocatalytic efficiency between ACF/TiO₂ and Fe-ACF/TiO₂. (% removal of model dye (photodegradation) = $(C_{pT}/C_0) \times 100\%$ where C_0 = concentration of model pollutant at 0 min, C_{pT} = concentration of model pollutant at experimental time). According to Fig. 5, the photoabsorbance of the samples increased upon introducing the Fe component, and the visible light absorbance of FT2 composite reached its maximum value.

As shown Eqs (5)-(6), Fe (III) mainly served as an OH⁻ trap. First, the produced OH ions were trapped on Fe (III) ion sites, and were subsequently combined with Fe (III) to form superoxide radical ion OH⁻. Otherwise, Fe (III) ion can act as an electron trap at

the same time, the recombination of the photoexcited charge carriers in the nanostructure can be restrained by Fe (III) ion. The baleful transfer of electrons can reduce photonic activity when the excess concentration of Fe was contained. The reaction was showed in the eqs (7), between FT2 and FT3, the curve of MB degradation of FT3 sample was some lower than that of FT2 sample due to this effect of Eqs (7).



Although photon energy of TiO₂ can be high excited under UV light, but after introduction of Fe species to TiO₂ lattices, improved lower energy under visible light. In comparison of non-treated ACF/TiO₂ and Fe-treated ACF/TiO₂, the degradation activity was enhanced due to introduction of Fe. Based on the reported studies and our work on Fe treated-ACF/TiO₂ photocatalyst composites, efforts were made to elucidate the mechanism of OH⁻ trap of Fe, which is depicted in Fig. 6. The possible mechanism for MB photonic activity by Fe-ACF/TiO₂ composites was as follows:

- (1) Photons of visible range were first absorbed by Fe-ACF/TiO₂ due to narrow band gap.
- (2) MB molecules acts as an electron donor, donates electron to conduction band (CB).
- (3) Excited electron is now available for degradation of MB and derivative of hydrogen peroxide at the same time.
- (4) Iron presented in the solution acts as a hydroxyl recipient, combines hydroxyl to become hydroxyl

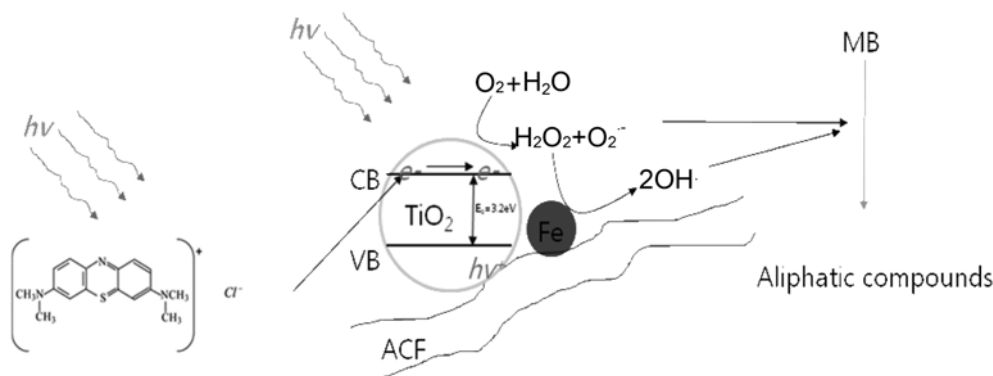


Fig. 6. The mechanism of OH⁻ trap of Fe.

radicals.

(5) Although the band gap energy of Fe-ACF/TiO₂ under visible light is less. Hydroxyl is very suitable transfer due to introduction of Fe species. It's one kind of reason to achieve a higher photonic reaction.

4. Conclusions

In this work, TiO₂ catalysts loaded on Fe-ACF support were prepared by a sol-gel method. From the SEM images, it was clear that the particles of TiO₂ and the structure of ACF, and the particles of TiO₂ aggregated into clusters were fixed on the surface of ACF. XRD patterns of the composites showed that the Fe-treated ACF/TiO₂ contained a mixing anatase and rutile phase. The EDX spectra showed the main peaks of C, O, Ti and Fe. Finally, higher degradation activity was obtained in case of the preparation of composite under visible light. It can be explained that the Fe-treated ACF/TiO₂ improved the unique OH ions transfer and the interfacial charge transfer to achieve a higher photonic activity.

References

1. M. R. Hoffmann, S. T. Martin, W. Y. Choi and D. W. Bahnemann, *Chem. Rev.*, **95**, 69-96(1995).
2. A. L. Linsebigler, G. Q. Lu and J. T. Yates Jr, *Chem. Rev.*, **95**, 735-758(1995).
3. N. Negishi, T. Iyoda, K. Hashimoto and A. Fujishima, *Chem. Lett.*, **24**, 841-843(1995).
4. I. Sopyan, M. Watanabe and S. Murasawa, *Chem. Lett.*, **1**, 69-71(1996).
5. T. Torimoto, S. Ito, S. Kuwabata and H. Yoneyama, *Environ. Sci. Technol.*, **30**, 1275-1281(1996).
6. A. Mills and S. L. Hunte, *J. Photochem. Photobiol. A: Chem.*, **108**, 1-35(1997).
7. A. Fujishima, T. N. Rao and D. A. Tryk, *J. Photochem. Photobiol. C: Photochem. Rev.*, **1**, 1-35(2000).
8. J. Matos, J. Laine and J. M. Herrman, *Appl. Catal. B: Environ.*, **18**, 281-291(1998).
9. S. X. Liu, Z. P. Qu, X. W. Han and C. L. Sun, *Catal. Today*, **93**, 877-884(2004).
10. T. Sauer, G. C. Neto, H. J. Jose and R. F. P. M. Moreira, *J. Photochem. Photobiol. A: Chem.*, **149**, 147-154(2002).
11. C. Galindo, P. Jacques and A. Kalt, *J. Photochem. Photobiol. A: Chem.*, **141**, 47-56(2001).
12. F. Zhang, J. Zhao, T. Shen, H. Hidaka, E. Pelizzetti and N. Serpone, *Appl. Catal. B: Environ.*, **15**, 147-156(1998).
13. M. A. Hasnat, I. A. Siddiquey and A. Nuruddin, *Dyes Pigments*, **66**, 185-188(2005).
14. R.W. Matthews, *J. Phys. Chem.*, **91**, 3328-3333(1987).
15. W. Zhao, C. C. Chen, X. Z. Li and J. C. Zhao, *J. Phys. Chem. B.*, **106**, 5022-5028(2002).
16. W. D. Wang, P. Serp, P. Kalck and J. Luy's Faria, *J. Molecular Catal A: Chem.*, **235**, 194-199(2005).
17. W. Choi, A. Termin and M. Hoffmann, *J. Phys. Chem.*, **98**, 13669-13679(1994).
18. W. Shockley and W. T. Read, *J. Phys. Rev.*, **87**, 835-842(1952).
19. A. Asahi, T. Morikawa, T. Ohwaki, K. Aoki and Y. Taga, *Sci.*, **293**, 269-271(2001).
20. Y. B. Xie and C. W. Yuan, *Appl. Catal. B: Environ.*, **46**, 251-259(2003).
21. Y. B. Xie and C. W. Yuan, *Appl. Surf. Sci.*, **221**, 17-24(2004).
22. L. C. Chena, Y. C. Hoa, W. S. Guo, C. M. Huang and T. C. Pan, *Electrochimica. Acta*, **54**, 3884-3891(2009).
23. B. Pal, M. Sharon and G. Nogami, *Mater. Chem. Phys.*, **59**, 254-261(1999).
24. Z. M. Wang, G. Yang, P. Biswas, W. Bresser and P. Boolchand, *Powder. Technol.*, **114**, 197-204(2001).
25. W. C. Oh and M. L. Chen, *J. Ceram. Process. Res.*, **9**, 100-106(2008).
26. M. L. Chen, S. Lim and W. C. Oh, *Carbon. Lett.*, **8**, 177-183(2007).
27. Y. G. Go, F. J. Zhang, M. L. Chen and W. C. Oh, *J. Mater. Res.*, **19**, 142-150(2009).
28. I. Konstantinou and T. Albanis, *Appl. Catal. B: Environ.*, **42**, 319-335(2003).
29. M. Inagaki, Y. Hirose, T. Matsunage, T. Tsumura and M. Toyoda, *Carbon*, **41**, 2619-2642(2003).
30. M. L. Chen, J. S. Bae and W. C. Oh, *Analytical. Sci. Technol.*, **19**, 460-467(2006).
31. B. Tryba, A. W. Morawski and M. Inagaki, *Appl. Catal. B: Environ.*, **46**, 203-208(2003).
32. K. Nagaveni, M. S. Hedge and G. Madras, *J. Phys. Chem. B.*, **108**, 20204-20212(2004).